Carbohydrate Polymers 86 (2011) 1244–1251

Contents lists available at ScienceDirect

Carbohydrate Polymers

journal homepage: www.elsevier.com/locate/carbpol

Organically modified nanosized starch derivatives as excellent reinforcing agents for bionanocomposites

Mayur Valodkar, Sonal Thakore*

Department of Chemistry, Faculty of Science, The M. S. University of Baroda, Vadodara 390002, India

ARTICLE INFO

Article history:
Received 20 December 2010
Received in revised form 24 May 2011
Accepted 8 June 2011
Available online 15 June 2011

Keywords:
Nanocomposites
Stress/strain curves
Thermal properties
Dynamic mechanical thermal analysis
Transmission electron microscopy

ABSTRACT

Organic modification of starch nanoparticles was carried out at room temperature to obtain nanosized hydrophobic derivatives. The particle size of the modified starch nanoparticles obtained by transmission electron microscopy (TEM) and X-ray diffraction (XRD) was found out to be around 50 nm. The hydrophobic starch derivatives were used to prepare bionanocomposites of natural rubber by mastication process. The properties were compared with composites obtained from untreated starch nanoparticles and carbon black. Up to 30 phr of the fillers were successfully incorporated leading to an enhancement in mechanical as well as thermal properties. Scanning electron microscopy (SEM) revealed single phase morphology of nanobiocomposites indicating compatibility of the filler and matrix. Dynamic mechanical properties were seen as a broad tan delta peak over a large range of temperature. It was observed that modified starch nanoparticles could be a potential substitute for carbon black as reinforcing agents and as promising materials for vibration damping applications.

1. Introduction

Polymer nanocomposites successfully integrate the two concepts of composites and nanometer sized materials. It is accepted that the term 'nanocomposites' describes a class of two-phase materials where one of the phases has at least one dimension lower than 100 nm (Bendahou, Kaddami, & Dufresne, 2010). Due to nanometric size effect these composites display some unique outstanding properties with respect to their conventional microcomposite counterparts. Polysaccharides such as cellulose, starch and chitin are a potential renewable source of nanosized reinforcement. They are naturally found in a semicrystalline state. Aqueous acids can be employed to hydrolyze the amorphous sections of the polymer. As a result the crystalline sections of these polysaccharides are released, resulting in individual monocrystalline nanoparticles (My Ahmed Said Azizi, Alloin, & Dufresne, 2005). The concept of reinforced polymer materials with polysaccharide nanofillers has known rapid advances and considerable interest in the last decade owing to their renewable character, high mechanical properties, low density and diversity of the sources (Bendahou et al., 2010). The use of starch nanoparticles is receiving a significant amount of attention because of the abundant availability of starch, low cost, renewability, biocompatibility, biodegradability and non-toxicity (Chakraborty, Sahoo, Teraoka, Miller, & Gross, 2005). Starch nanocrystals obtained by acid hydrolysis of waxy maize starch have been used as filler in a synthetic polymeric matrix and appeared to be an interesting reinforcing agent (Angellier, Molina-Boisseau, Putaux, Dupeyre & Dufresne, 2005; Dufresne & Cavaille, 1998; Dufresne, Cavaille, & Helbert, 1996). In this context, waxy maize starch nanocrystals have been considered as potential filler for natural rubber (NR), which is one of the most important elastomers widely used in industrial and technological areas (Thakore, Desai, Sarawade, & Devi, 2001). However most of the composites have been prepared by solution blending.

We have mainly concentrated on studying the reinforcement ability of starch by employing commercial mixing methods. Both native starch as well as starch nanoparticles are found to induce excellent reinforcement in natural rubber (Thakore et al., 2001; Valodkar & Thakore, 2010, in press). The main hurdle for the use of starch as a reinforcing phase is its hydrophilicity. Hence, there is a growing interest in organically modified derivatives of polysaccharides for different applications (Thielemans, Belgacem, & Dufresne, 2006; Tsuji & Kawaguchi, 2005; Xu et al., 2010). The amphiphillic nature imparted upon polysaccharides after hydrophobic modification gives them a wide and interesting applications spectrum, for instance as rheology modifier, emulsion stabilizer, surface modifier and as drug delivery vehicles. Chemical modification of starch nanocrystals is reported with various reagents such as anhydrides and fatty acids in organic and aqueous solvents (Namazi & Dadkhah, 2010; Namazi, Mosadegh, & Dadkhah, 2009; Wang et al., 2009). Modification also has been done

* Corresponding author. Tel.: +91 0265 2795552; fax: +91 0265 2429814.
E-mail address: chemistry2797@yahoo.com (S. Thakore).

0144-8617/$ – see front matter © 2011 Elsevier Ltd. All rights reserved.
doi:10.1016/j.carbpol.2011.06.020

via graft polymerization of caprolactone, poly ethylene oxide, etc. (Fang, Fowler, Tomkinson, & Hill, 2002; Namazi & Dadkhah, 2010; Namazi et al., 2009; Thielemans et al., 2006; Tsuji & Kawaguchi, 2005; Wang et al., 2009; Xu et al., 2010). However most of these modifications require drastic or prolonged reaction conditions which may also lead to agglomeration of the starch nanocrystals.

Hence we preferred to carry out room temperature organic modification of starch nanoparticles obtained by acid hydrolysis. The resulting hydrophobic derivatives were used for the development of bionanocomposite of natural rubber by commercial mastication process. Mastication process is superior because (i) it is environmentally safe due to the absence of organic solvents and (ii) it is compatible with the current industrial process such as extrusion and injection molding. A comparison was made with mechanical and thermal properties of conventional composite counterparts.

2. Experimental

2.1. Materials

Waxy maize starch (containing mostly amylopectin and small traces of amylose), sulfuric acid, 1,4-hexamethylene diisocynate, dibutyl tin dilaureate (DBTDL), acetic anhydride, tetrahydrofuran (THF), toluenesulphonic acid (PTSA) and acetic acid were purchased from Sigma–Aldrich, Bombay. NR and carbon black (CB) were kindly supplied by Mouldtech Rubber Industries, Vadodara.

2.2. Preparation of starch nanoparticles (SNPs)

A given weight of waxy maize starch (SW) was mixed with 3.16 M H_2SO_4. The suspension was continuously stirred for 5 days. It was then washed by successive centrifugation in distilled water until neutrality. SNPs were stored at 4 °C with several drops of chloroform.

2.3. Isocynate modification of SNP (SNI)

The isocyanate modification was carried out as reported elsewhere (Valodkar & Thakore, 2010a). Previously dried SNP (1 mole) and HMDI (1.1 mole) were allowed to react in dry tetrahydrofuran (THF) at room temperature in the presence of catalytic amount of DBTDL under nitrogen atmosphere to form a urethane linkage. The mixture was immediately subjected to ultrasonication to obtain a homogeneous dispersion of isocyanate modified starch nanoparticles in THF. Subsequent lyophilization of the dispersion resulted in dried nanoparticles.

2.4. Acetylated SNP (SNAC)

SNPs and acetic acid were mixed at room temperature. Acetic anhydride was added dropwise to the above mixture. After stirring for few minutes PTSA was added and the reaction mass was stirred for 6 h at 60 °C. The product was filtered and dried at 50 °C under vacuum. Degree of substitution was determined to be 2.7.

2.5. Preparation of bionanocomposites

The bionanocomposites of NR were prepared on two roll mixing mill. The mastication was continued until homogenous composites were obtained. This was followed by vulcanization at 150 °C and ~300 kPa pressure for 7–8 min to obtain rubber composite sheets with 1 mm thickness.

Four sets of bionanocomposites were synthesized using each of waxy corn starch (SW), starch nanocrystals (SNP), HMDI modified starch nanoparticles (SNI) and acetylated starch nanoparticles (SNAC) as reinforcing fillers in NR. Up to 30 phr of fillers were added along with the accelerators such as sulphur (1.8 phr), tetramethylene thiuram disulphide (0.5 phr), mercaptobenzo thiazyl disulphide (1 phr), zinc oxide (5 phr), and stearic acid (1 phr). Composites with carbon black (CB/NR) were also prepared for comparison.

2.6. Characterization of nanoparticles

Size and shape of the nanoparticles were determined by using TEM on a Philips, Holland Technai 20 model operating at 200 kV. The sample for TEM was prepared by putting one drop of the colloidal copper solution onto standard carbon-coated copper grids and then drying under an electric bulb for 30 min. X-ray diffraction (XRD) was determined by using PANalytical 'X'PERT-PRO XRPD. FT-IR spectra of starch and the vacuum dried nanoparticles were recorded as the KBr pellet on the Perkin Elmer RX1 model.

2.7. Characterization of nanocomposites

Stress/strain properties of all the NR composites were measured on a Universal Testing Machine (UTM, Lloyd Instrument) using test specimen in the form of dumbbells according to ASTM standard and procedure (D638). The gauge length was 50.0 mm. The crosshead speed was 10 mm/min at 25 °C and 50% humidity. The data given are the average of five measurements. The surface morphology of the tensile fractured surfaces was examined by means of Jeol Scanning Electron Microscope (JEOL JSM–5610LV). An accelerating potential of 15 kV was used for the analysis of the sample. TGA was recorded on TG–DTA 6300 INCARP EXSTAR 6000 in nitrogen atmosphere in temperature range of 30–450 °C at heating rate of 10 °C/min. DSC was performed on DSC 60 Shimadzu in nitrogen atmosphere in temperature range of −80 to 0 °C at heating rate of 10 °C/min. Dynamic mechanical tests were carried out using NETZSCH DMA 242. The specimen was a thin rectangular strip ($15 \times 5.1 \times 0.959$). The range of temperature in which the analysis was carried out between −80 and 0 °C at the frequencies of 1, 5 and 10 Hz in nitrogen atmosphere. The setup measured the complex tensile modulus E^*, i.e., the storage component E' and the loss component E''. The ratio between the two components, $\tan\delta$ was also determined.

3. Results and discussion

Fig. 1A shows TEM images of nanocrystals before (Fig. 1A(a)) and after modification (Fig. 1A(b) and A(c)). After acid treatment process, the native waxy corn starch granules have been destructured and degraded to nanocrystals with a size range of 70–100 nm (Fig. 1A(a)). We did not recognize anymore the platelet shape of unmodified starch particles along with its crystallinity as revealed by XRD. The particles are more individualized and monodispersed than their unmodified counterparts with a size of 50 nm in case of SNI and 40 nm in case of SNAC. The starch nanoplatelets are believed to aggregate as a result of hydrogen bond interactions due to the surface hydroxyl groups (Valodkar & Thakore, 2010b). Blocking these interactions by relatively large molecular weight molecules obviously improves the individualization of the nanoparticles. The decrease in the polar contribution reduces the strength of the interparticle interactions and results in the individualization of the nanoplatelets (Valodkar & Thakore, 2010a).

Fig. 1B shows the XRD pattern of starch and starch modified nanoparticles. The diffraction pattern displays typical peaks of A-type amylose allomorph (Valodkar & Thakore, 2010b). It was characterized by peaks at 2 theta value at 11.23° (0.76 nm) and

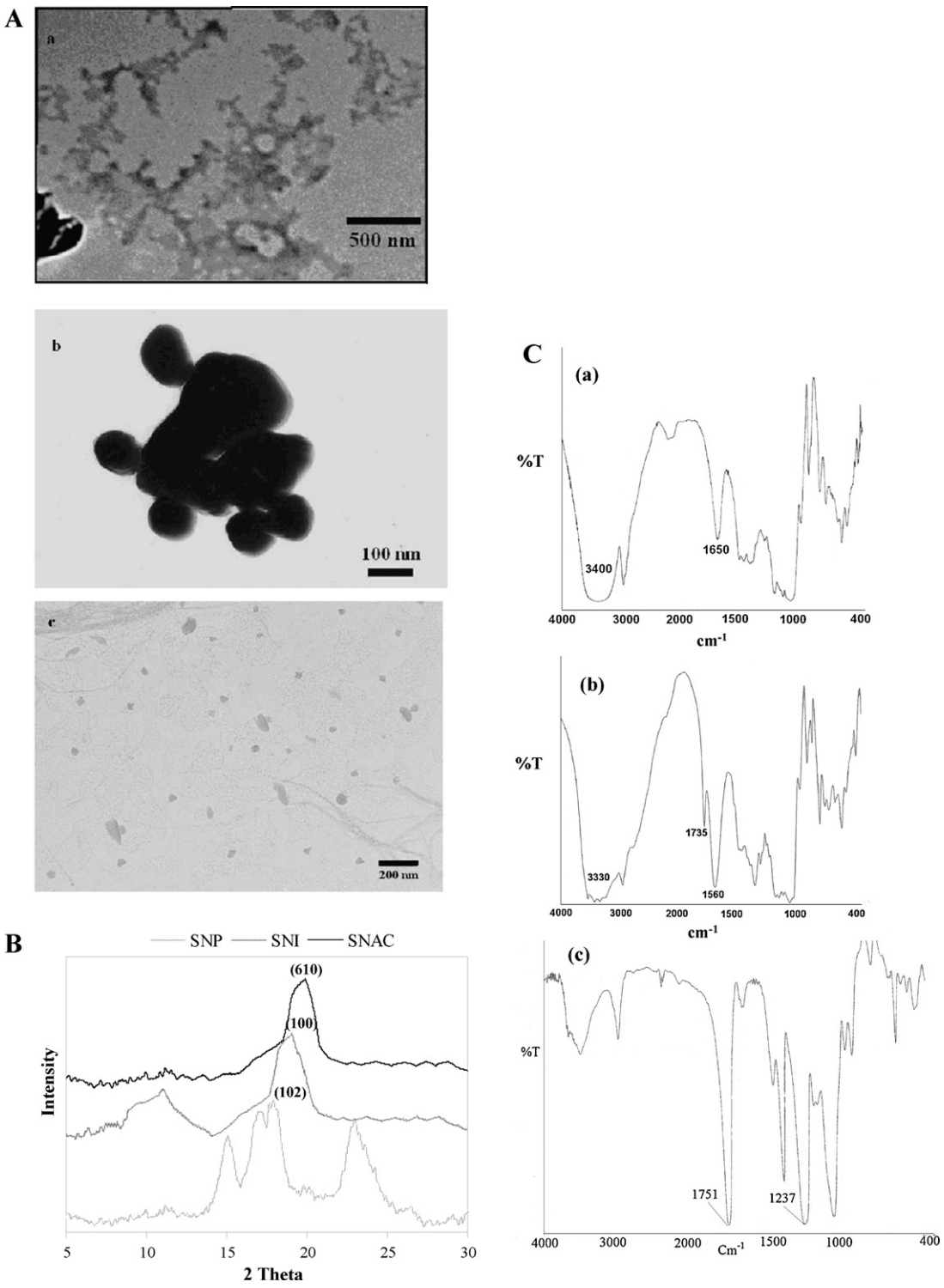

Fig. 1. (A) TEM images, (B) XRD spectra and (C) FT-IR spectra of nanoparticles: (a) SNP, (b) SNI and (c) SNAC.

a peak at 15.03° and 22.99°, and double strong peak at 17.2° and 17.97°. While in case of modified SNP i.e. SNI and SNAC, A-style crystallinity of SNPs was destroyed and a peak at 11° and 19° were observed in case of SNI whereas in case of SNAC peak at 21° was observed (Xu, Miladinov, & Hanna, 2004). This indicates that all the hydroxyl groups of SNP are replaced by isocyanate and acetyl group and no intermolecular hydrogen bonding was formed which destroy the ordered crystallinity. The average particle size calculated from the width of the reflection according to the Debye–Scherrer equation (Eq. (1)) of SNP, SNI and SNAC was about 65 nm, 42 nm and 34 nm respectively.

$$D(\text{nm}) = \frac{K\lambda}{\beta \cos \theta} \quad (1)$$

where K is a constant equal to 0.89, λ is the X-ray wavelength (1.54 Å), β is the full-width at half-maximum (fwhm) of the major peak expressed in radians, and θ is the Bragg angle (deg) corresponding to that peak.

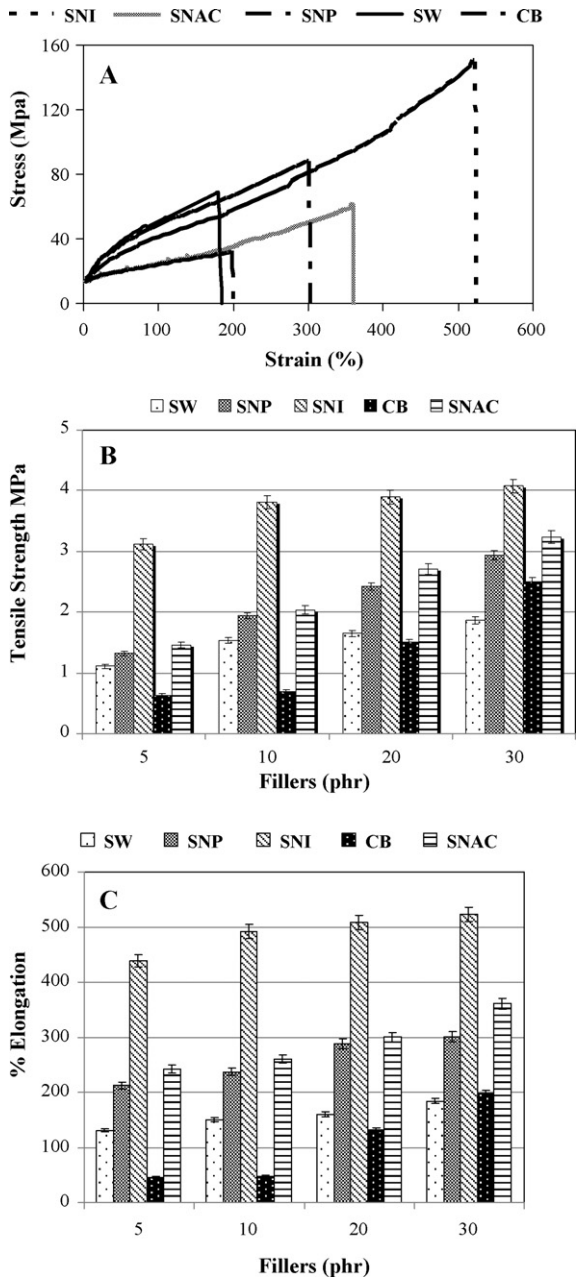

Fig. 2. Effect of various fillers on (A) stress–strain curve of nanocomposites at 30 phr loading, (B) tensile strength and (C) % elongation.

Fig. 1C shows the FT-IR spectra of nanoparticles. In the spectra of SNP the peak at 3400 cm^{-1} was due to –OH stretching and peak at 1650 cm^{-1} was due to tightly bound water (Valodkar & Thakore, 2010a). While absorption band between 1000 and 1200 cm^{-1} were characteristic of the –C–O stretching of polysaccharide skeleton. In case of SNI the characteristic carbonyl stretching of urethane linkage was observed at 1735 cm^{-1}. The absorptions resulting from –NH stretching and bending vibration were observed at 3330 and 1560 cm^{-1} (Valodkar & Thakore, 2010b). In acetylated starch nanoparticle a strong absorption peak at 1751 cm^{-1} was attributed to stretching of ester carbonyl –C=O (Valodkar & Thakore, 2010a). The peak at 3400 almost disappeared indicating that the degree of substitution is close to 3. The other peak at 1237 cm^{-1} was attributed to C–O–C– bond stretching of ether linkage.

Typical stress vs. strain curves for the NR nanocomposites at 30 phr are shown in Fig. 2A. For each measurement, it was observed that the strain was macroscopically homogenous and uniform along the sample until it breaks. The lack of any necking phenomenon confirms the homogenous nature of these nanocomposites. The samples exhibit an elastic behavior at $T > T_g$. The stress continuously increases with strain and the amount of fillers as shown in Fig. 2A. Incorporation of nanofillers leads to an increase in strength as well as elongation at break. Whereas Angellier, Molina-Boisseau, and Dufresne (2005) observed decrease in elongation as the amount of filler increases. The behavior is consistent with respect to all the nanofillers. Thus we can say that the nanofillers used retains the elastic property of natural rubber which is also concluded by dynamic mechanical analysis (in the later section). The initial high stress is due to the reinforcement of the rubber with nanofillers (Varghese & Karger-Kocsis, 2003). As the strain increases, stress induced crystallization comes into role, which increases proportionally along with strain (Varghese & Karger-Kocsis, 2003). The dispersion of nanofillers leads to an efficient reinforcement, which leads to improved stiffness. The unmodified starch nanoparticles (SNP) showed lower strength as compared to modified starch nanoparticles. Due to hydrophilic nature of SNP and hydrophobic nature of NR the adhesion between the two is poor. As a result the stress transfer from the matrix to the filler is poor and the mechanical properties of nanoparticles are not fully utilized.

It can be seen from Fig. 2B that as the amount of nanofillers increases the tensile strength (T.S.) goes on increasing as expected. It follows the order SNI/NR > SNAC/NR > SNP/NR > SW/NR. In case of CB composites the initial lower T.S. value rapidly increases from 10 to 30 phr loading but remains lower than nanocomposites at all levels. Nanocomposites of modified SNPs showed greater strength and elongation due to their improved dispersion and better compatibility with NR due to its hydrophobic nature and small particle size. Among the modified SNPs, SNI showed higher mechanical properties which can be explained on the basis of chemical reactions that are likely to occur during the process of vulcanization. At this high temperature the free NCO groups of isocyanate terminated SNIs may react further to form three-dimensional allophanate or biuret crosslinks or polar urea structure thus leading to increased chemical crosslinking (Desai, Thakore, Sarawade, & Devi, 2000) which imparts higher mechanical strength to the nanocomposite.

Fig. 2C shows that as the amount of nanofillers in NR goes on increasing the elongation increases along with T.S. which is also seen in CB composites. This is an interesting observation as generally elongation and T.S. show opposite trend. Also the increase in % elongation in case of modified SNP is more progressive than CB composites. High nanofiller content seems to preserve the elastic behavior of NR-based nanocomposites. In case of SW/NR the increase is obtained because it has high amylopectin content and hence higher molecular weight. SW imparts lower mechanical strength than other nanofillers due to poor compatibility with hydrophobic NR.

The increase in tensile strength with addition of modified starch has also been reported by Wang et al. (2009) for xanthate derivative of cassava starch. In the present investigation the value for tensile strength and % elongation for unfilled rubber are 0.58 MPa and 41% respectively. Our values of tensile strength are much lower than those reported by Wang et al. which may be because we report ultimate tensile strength. The values of ultimate tensile strength are always lower than true tensile strength. Further the method of preparation of the composites is also entirely different. However the difference between unfilled and filled composites is much higher in our case. The use of modified starch nanoparticles showed up to 700% increase in T.S. in our case as compared to 130% increase in case of starch xanthate. The decrease in size of starch is also quite evident. At 10% loading starch nanoparticles lead to an increase of 330% against 105% increase observed by Wang et al. for cassava starch. Another important feature is the synergistic increase

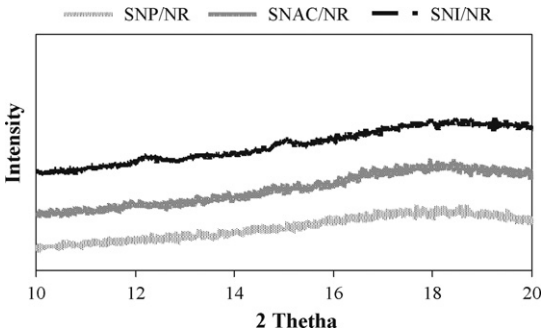

Fig. 3. XRD spectra of nanocomposites at 30 phr loading.

tensile strength as well as elongation in the bionanocomposites under study. Thus our study reflects a combined effect of reduction in size as well as organic modification.

The XRD of nanocomposites at 30 phr loading (Fig. 3) showed no diffraction peak corresponding to pure NR unlike other reports (Qu et al., 2009; Pojanavaraphan & Magaraphan, 2008; Mondragon, Hernandez, Rivera-Armenta, & Rodriguez-Gonzalez, 2009). This is because the filler loadings in the present case are much higher than those reported by Huang et al., Mondragon et al. and Pojanavaraphan et al. for nanoclays (10 phr or less). On the other hand, for high filler loadings Dufresne et al. have observed that the processing by casting and evaporation at 40 °C did not affect the crystallinity of starch in nanocomposite (Angellier, Molina-Boisseau, & Dufresne, 2005). While the vulcanization process in the present case may have led to change in the structure of the nanocrystals from crystalline to amorphous. This accounts for the absence of peaks corresponding to modified and unmodified starch in XRD of present nanocomposites.

The results of the mechanical properties can be explained on the basis of morphology. The SE micrographs of fractured samples of biocomposites at 30 phr loading are shown in Fig. 4(A)–(E). It can be seen that all the bionanofillers are well dispersed into polymer matrix without much agglomeration. Uniform distribution of modified and unmodified SNP into NR matrix is observed. This is due to the compatibility between the modified SNP and the NR matrix (Fig. 4A and B). While in case of unmodified SNP the reduction in size compensates for the hydrophilic nature (Fig. 4C), in case of waxy maize starch (SW) it seems to be lack of interfacial adhesion. The lack of any evidence of agglomeration combined with the significant increase in mechanical properties indicates even distribution of nanofillers in NR. In case of CB composites (Fig. 4E) relatively coarse, two-phase morphology is seen.

Typical TG curves (supplementary data) of the nanocomposites at 30 phr loading showed an initial mass loss from temperature 150–250 °C attributed to elimination of volatile components such as water (Dufresne et al., 1996). At 350 °C the percentage of weight retained is higher for nanocomposite (Table 1). This increase in thermal stability of the hybrid may result from the dispersion of the nanoparticles and strong interaction between the nanoparticles and rubber molecules. High vulcanization temperatures may have resulted in crosslinking within the polysaccharide network which led to unusual thermal stability of the nanocomposites.

Table 1
TG values of bionanocomposites of NR.

Fillers	Degradation temperature for wt.% loss					Activation energy E_a (kJ/mol)
	1	2	5	10	50	
SW	128	179	250	303	371	33.23
SNP	135	198	276	305	375	54.17
SNI	203	255	310	336	378	57.61
SNAC	170	231	292	326	376	56.32
CB	114	192	264	304	364	29.10

Table 2
DMA data for bionanocomposites.

Fillers	T_g °C	Activation energy E_a (kJ/mol)
SNP	−55	312.61
SNI	−50	369.81
SNAC	−48	324.75

DSC curves of NR composites at 30 phr filler loading (Supplementary Data) show that all the nanocomposites have T_g comparable with that of CB/NR composites. While that of unfilled NR is around −66 °C (Dufresne et al., 1996). The T_g also goes on increasing with the nanofillers loading as expected. The T_g of SNI/NR is highest followed by SNAC/NR, SNP/NR, SW/NR and CB/NR composites. The results of thermal properties support the observation that increased hydrophobicity and reduced particle size of filler imparts rigidity and strength to the network. Also isocynate modification leads to a greater increase in T_g due to increased crosslinking as already explained for enhanced mechanical strength.

Fig. 5 depicts the dynamic mechanical spectra (logarithm of dynamic storage modulus $\log(E')$ and loss factor ($\tan\delta$)) as a function of temperature for the nanocomposites at 1 Hz. A sharp decrease over 3 decades is observed around −60 °C, corresponding to the primary relaxation process associated with the glass–rubber transition determined by differential scanning calorimetry (DSC) measurements. This modulus drop corresponds to an energy dissipation phenomenon displayed in the concomitant relaxation process where $\tan\delta$ passes through a maximum. Dynamic mechanical analysis involves weak stresses, the adhesion between the filler and the matrix is not damaged. Under higher stress, as used for tensile tests, the adhesion is involved. Nanocomposites obtained similar $\tan\delta$ curve as that of Teh, Mohd Ishak, Hashim, Karger-Koesis, and Ishiaku (2004). The $\tan\delta$ curve of nanocomposites showed a broad relaxation process from −80 °C to −10 °C. This may be due to the relaxation of rubber fraction confined inside the layers. The reduction in the $\tan\delta$ maxima suggests a strong adhesion between NR and modified starch nanoparticles. Sliding along the exfoliated interlayer is suppressed. In addition, chain slipping at the outer surfaces of the aggregates is likely also hampered. Therefore the loss maximum is smallest in case of the nanocomposites system with the strongest filler matrix coupling (Varghese & Karger-Kocsis, 2003). Mondragon et al. (2009) observed that E' increases with clay content above T_g which shows that the clay content affects the elastic properties associated to the rubber phase. Whereas in the present study the values of E' does not increase with the filler loading above T_g. This indicates that the nanofillers does not affect the elastic properties associated to the rubber phase. The T_g values of DSC somewhat differ from DMA. This may be attributed to the frequency dependence of transition phenomenon. The activation energy (Table 2) for glass transition was calculated from following Eq. (2) (Desai, Thakore, Brennan, & Devi, 2001).

$$\ln\frac{\omega_1}{\omega_2} = \frac{E_a}{R(1/T_2 - 1/T_1)} \quad (2)$$

3.1. Sorption studies

Water and toluene uptake was determined by a method reported elsewhere (Valodkar & Thakore, 2010b). Absorption largely depends on the hydrophobic or hydrophilic components embedded in the matrix, which acts as a semipermeable membrane. The fiber/matrix adhesion is an important factor

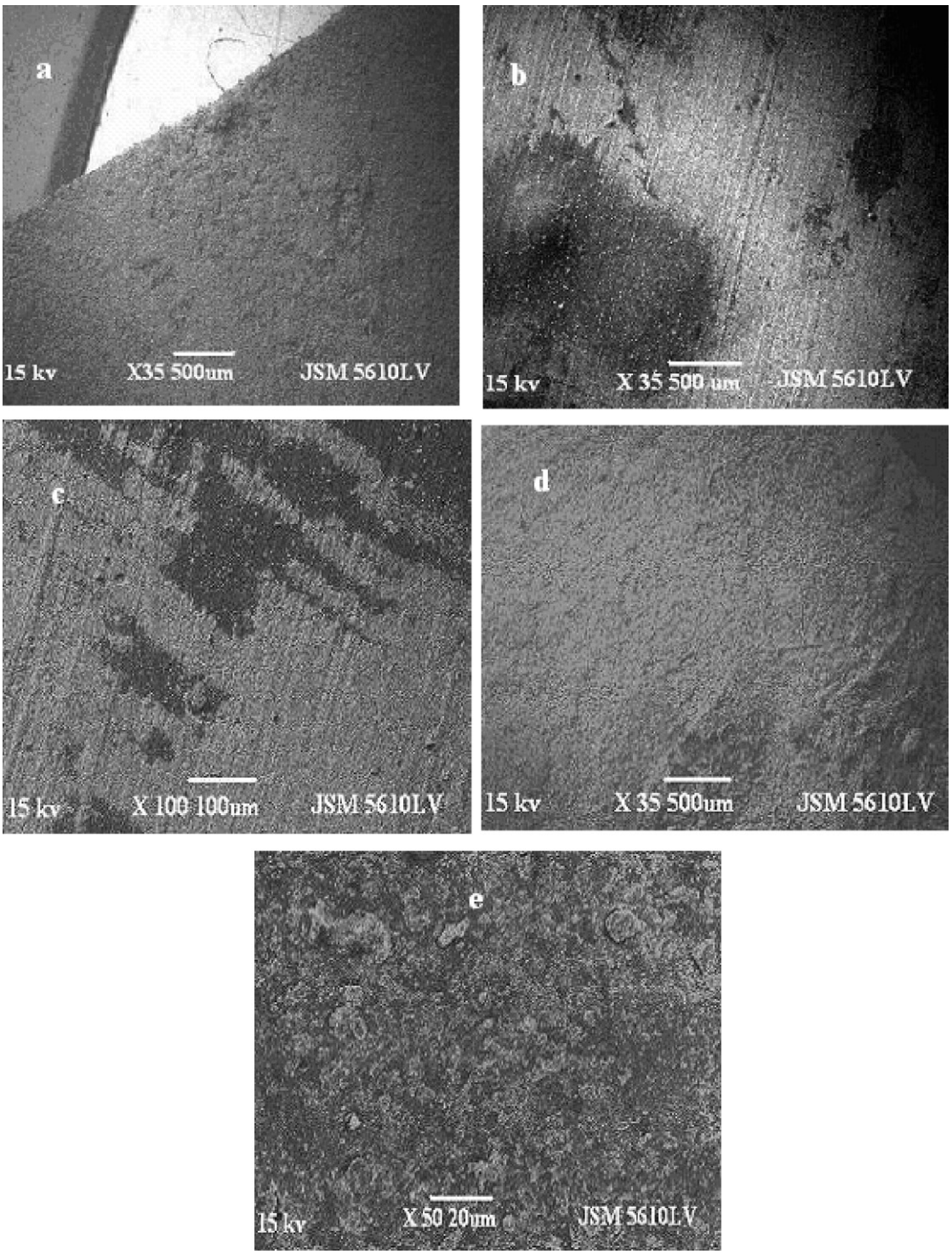

Fig. 4. SE Micrographs of NR nanocomposites at 30 phr loading of (A) SNI, (B) SNAC, (C) SNP, (D) SW and (E) CB.

in determining the sorption behavior of a composite (Jacob, Varughese, & Thomas, 2005). Moreover, fiber architecture has also been found to affect the absorption. Sorption studies were performed in water and nonpolar solvent toluene in order to understand the degree of hydrophobicity. As the bionanofillers used here are polysaccharides the water sorption was expected to be high and proportional to filler loading. However the results of the experiment (Table 3) showed an interesting trend. The maximum water uptake even at 30% filler loading is 3.46% which is not significant. Further, the sorption values decrease with filler loading. The low sorption indicates increasing adhesion between the polymer matrix and filler. The interaction leads to the formation of a bound polymer in close proximity to the reinforcing filler, which restricts the solvent uptake. As the amount of filler loading increases, the amount of the bound polymer is lower and, consequently, the solvent uptake is lower. Also, the high curing temperatures may have introduced certain degree of crosslinking which also decreases the uptake. However the modified fillers led to decreased water sorption and increased toluene sorption of the nanocomposites which is well in agreement with their hydrophobic

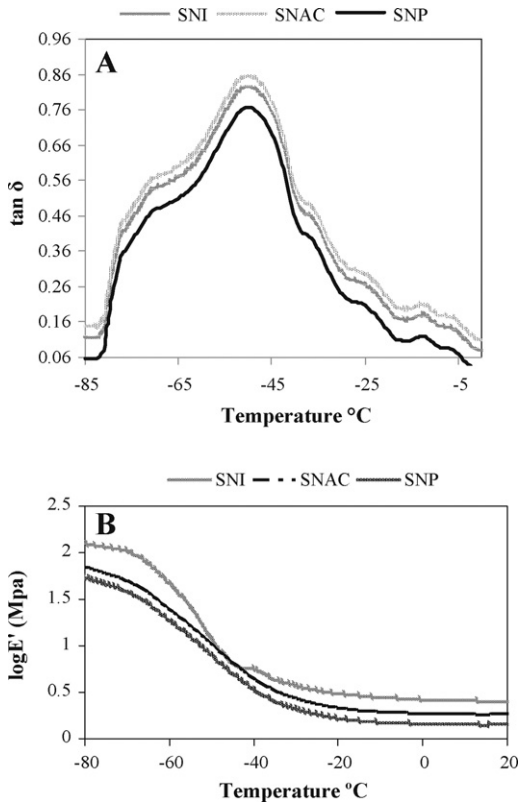

Fig. 5. Effect of nanocomposites on (A) mechanical loss factor tan δ and (B) logarithm of storage modulus E' vs. temperature.

Table 3
Water and toluene sorption of bionanocomposites.

Fillers	% mole uptake					
	Water			Toluene		
	10 phr	20 phr	30 phr	10 phr	20 phr	30 phr
SNI	0.98	0.37	0.21	2.73	2.39	2.06
SNAC	1.13	0.51	0.26	2.76	2.44	2.12
SNP	3.10	2.87	2.44	1.22	0.65	0.34
SW	3.46	2.81	2.51	1.30	0.82	0.60
CB	1.15	0.71	0.56	2.77	2.38	1.97

nature. The lower toluene sorption values of SNI also favour the greater crosslink density of SNI filled nanocomposites compared to SNAc/NR nanocomposites.

4. Conclusion

The room temperature chemical reaction led to successful synthesis of nanosized hydrophobic derivatives which could be incorporated in NR matrix up to 30 phr, by mastication process. All the bionanocomposites showed superior strength and elongation than conventional Carbon Black/NR composites at all loadings. The modified starch nanoparticles showed better compatibility with NR matrix as per the morphology and XRD studies of bionanocomposites which revealed the uniform morphology and nearly exfoliated structure. Isocyanate modified starch nanoparticles imparted highest strength, increased the T_g and decreased solvent sorption probably due to formation of additional crosslinks during vulcanization process. Despite the polysaccharide origin the starchy fillers did not deteriorate the thermal stability of the nanocomposites. The broad tan δ peak suggested high degree of compatibility of reinforcing fillers with NR matrix with potential application over a wide temperature range. The study opens up a new and green alternative for reinforcement of rubbers.

Acknowledgement

The authors are grateful to the University Grants Commission, New Delhi for financial assistance. Special thanks to Dr. Prasanna Ghalsasi Department of Chemistry for DSC studies and Dr. Vandana Rao Metallurgy Department, The M. S. University of Baroda, for SEM studies.

Appendix A. Supplementary data

Supplementary data associated with this article can be found, in the online version, at doi:10.1016/j.carbpol.2011.06.020.

References

Angellier, H., Molina-Boisseau, S., & Dufresne, A. (2005). Mechanical properties of waxy maize starch nanocrystal reinforced natural rubber. *Macromolecules*, *38*, 9161–9170.
Angellier, H., Molina-Boisseau, S., Putaux, J. L., Dupeyre, D., & Dufresne, A. (2005). Starch nanocrystals fillers in acrylic polymer matrix. *Macromolecular Symposium*, *221*, 95–104.
Bendahou, A., Kaddami, H., & Dufresne, A. (2010). Investigation on the effect of cellulosic nanoparticles morphology on the properties of natural rubber based nanocomposites. *European Polymer Journal*, *46*, 609–620.
Chakraborty, S., Sahoo, B., Teraoka, I., Miller, L. M., & Gross, R. A. (2005). Enzyme-catalyzed regioselective modification of starch nanoparticles. *Macromolecules*, *38*, 61–68.
Desai, S., Thakore, I. M., Sarawade, B. D., & Devi, S. (2000). Effect of polyol and diisocynate on thermo-mechanical and morphological properties of polyurethane. *European Polymer Journal*, *36*, 711–725.
Desai, S., Thakore, I. M., Brennan, A., & Devi, S. (2001). Polyurethane nitrile rubber blends. *Journal of Macromolecule Science Pure and Applied Chemistry A*, *38*, 711–729.
Dufresne, A., & Cavaille, J. Y. (1998). Clustering and percolation effects in microcrystalline starch-reinforced thermoplastic. *Journal of Polymer Science Part B Polymer Physics*, *36*, 2211–2224.
Dufresne, A., Cavaille, J. Y., & Helbert, W. (1996). New nanocomposite materials: Microcrystalline starch reinforced thermoplastic. *Macromolecules*, *29*, 7624–7626.
Fang, J. M., Fowler, P. A., Tomkinson, J., & Hill, C. A. S. (2002). Preparation and characterization of chemically modified potato starch. *Carbohydrate Polymers*, *47*, 245–252.
Jacob, M., Varughese, K. T., & Thomas, S. (2005). Water sorption studies of hybrid biofiber-reinforced natural rubber biocomposites. *Biomacromolecules*, *6*, 2969–2979.
Mondragon, M., Hernandez, E. M., Rivera-Armenta, J. L., & Rodriguez-Gonzalez, F. J. (2009). Injection molded thermoplastic starch/natural rubber/clay nanocomposites: Morphology and mechanical properties. *Carbohydrate Polymer*, *77*, 80–86.
My Ahmed Said Azizi, S., Alloin, F., & Dufresne, A. (2005). Review of recent research into cellulosic whiskers, their properties and their application in nanocomposite field. *Biomacromolecules*, *6*, 612–626.
Namazi, H., & Dadkhah, A. (2010). Conventional method for preparation of hydrophobically modified starch nanocrystals with using fatty acids. *Carbohydrate Polymers*, *79*, 731–737.
Namazi, H., Mosadegh, M., & Dadkhah, A. (2009). New intercalated layer silicate nanocomposites based on synthesized starch-g-PCL prepared via solution intercalation and in situ polymerization method: As a comparative study. *Carbohydrate Polymers*, *75*, 665–669.
Pojanavaraphan, T., & Magaraphan, R. (2008). Prevulcanized natural rubber latex/clay aerogel nanocomposites. *European Polymer Journal*, *44*, 1968–1977.
Qu, L., Huang, G., Liu, Z., Zhang, P., Weng, G., & Nie, Y. (2009). Remarkable reinforcement of natural rubber by deformation induced crystallization in the presence of organophilic montmorillonite. *Acta Materialia*, *57*, 5053–5060.
Teh, P. L., Mohd Ishak, Z. A., Hashim, A. S., Karger-Koesis, J., & Ishiaku, U. S. (2004). Effects of epoxidized natural rubber as a compatibilizer in melt compounded natural rubber organoclay nanocomposites. *European Polymer Journal*, *40*, 2513–2521.
Thakore, I. M., Desai, S., Sarawade, B. D., & Devi, S. (2001). Studies on biodegradability, morphology and thermomechanical properties of LDPE/modified starch blends. *European Polymer Journal*, *37*, 151–160.
Thielemans, W., Belgacem, M. N., & Dufresne, A. (2006). Starch nanocrystals with large chain surface modification. *Langmuir*, *22*, 4804–4810.
Tsuji, S., & Kawaguchi, H. (2005). Self assembly of poly(N-isopropylacrylamide)-carrying microsphere into two dimensional colloidal array. *Langmuir*, *21*, 2434–2437.

Valodkar, M., & Thakore, S. (2010a). Isocyanate crosslinked reactive starch nanoparticles for thermo-responsive conducting applications. *Carbohydrate Research*, *345*, 2354–2360.

Valodkar, M., & Thakore, S. (2010b). Thermal and mechanical properties of natural rubber and starch nanobiocomposites. *International Journal of Polymer Analysis and Characterisation*, *15*, 1–9.

Valodkar, M., & Thakore, S. Biocomposites as effective fillers in natural rubber: Composites v/s biocomposites. Journal of Applied Polymer Science, in press.

Varghese, S., & Karger-Kocsis, J. (2003). Natural rubber based nanocomposites by latex compounding with layered silicates. *Polymer*, *44*, 4921–4927.

Wang, Z. F., Peng, Z., Li, S. D., Lin, H., Zhang, K. X., She, X. D., et al. (2009). The impact of esterification on the properties of starch/natural rubber composite. *Composite Science and Technology*, *69*, 1797–1803.

Xu, Y., Ding, W., Liu, J., Li, Y., Kennedy, J. F., Gu, Q., et al. (2010). Preparation and characterization of organic-soluble acetylated starch nanocrystals. *Carbohydrate Polymers*, *80*, 1078–1084.

Xu, Y., Miladinov, V., & Hanna, M. A. (2004). Síntesis and characterization of starch acetales with high substitution. *Cereal Chemistry*, *81*, 735–740.